



# HHS Public Access

Author manuscript

*Nat Methods*. Author manuscript; available in PMC 2011 October 12.

Published in final edited form as:

*Nat Methods*. 2011 September ; 8(9): 737–743.

## MiMIC: a highly versatile transposon insertion resource for engineering *Drosophila melanogaster* genes

Koen J. T. Venken<sup>1,\*</sup>, Karen L. Schulze<sup>1,2</sup>, Nele A. Haelterman<sup>1</sup>, Hongling Pan<sup>1,2</sup>, Yuchun He<sup>1,2</sup>, Martha Evans-Holm<sup>3</sup>, Joseph W. Carlson<sup>3</sup>, Robert W. Levis<sup>4</sup>, Allan C. Spradling<sup>4</sup>, Roger A. Hoskins<sup>3</sup>, and Hugo J. Bellen<sup>1,2,5,6,\*</sup>

<sup>1</sup>Department of Molecular and Human Genetics, Baylor College of Medicine, Houston, TX 77030, USA

<sup>2</sup>Howard Hughes Medical Institute, Baylor College of Medicine, Houston, TX 77030, USA

<sup>3</sup>Life Sciences Division, Lawrence Berkeley National Laboratory, Berkeley, CA 94702, USA

<sup>4</sup>Department of Embryology, Howard Hughes Medical Institute, Carnegie Institution for Science, Baltimore, MD 21218, USA

<sup>5</sup>Department of Neuroscience, Baylor College of Medicine, Houston, TX 77030, USA

<sup>6</sup>Program in Developmental Biology, Baylor College of Medicine, Houston, TX 77030, USA

### Abstract

We demonstrate the versatility of a collection of insertions of the transposon *Minos* mediated integration cassette (MiMIC), in *Drosophila melanogaster*. MiMIC contains a gene-trap cassette and the *yellow*<sup>+</sup> marker flanked by two inverted bacteriophage  $\Phi$ C31 *attP* sites. MiMIC integrates almost at random in the genome to create sites for DNA manipulation. The *attP* sites allow the replacement of the intervening sequence of the transposon with any other sequence through recombinase mediated cassette exchange (RMCE). We can revert insertions that function as gene

---

Users may view, print, copy, download and text and data- mine the content in such documents, for the purposes of academic research, subject always to the full Conditions of use: [http://www.nature.com/authors/editorial\\_policies/license.html#terms](http://www.nature.com/authors/editorial_policies/license.html#terms)

\*Correspondence: kv134369@bcm.edu (K.J.T.V) and hbellen@bcm.tmc.edu (H.J.B.)

**AUTHOR CONTRIBUTIONS** K.J.T.V. designed the MiMIC technique.

R.W.L., A.C.S., R.A.H. and H.J.B. conceived the application of MiMIC to the Gene Disruption Project.

K.J.T.V. designed vectors and performed all molecular biology, except for mapping of insertions.

H.P. and Y.H. performed microinjections.

K.J.T.V., H.P. and Y.H. performed fly genetics.

M.E.-H. and R.A.H. performed inverse PCR and DNA sequencing to map insertions.

K.J.T.V., Y.H., M.E.-H., J.W.C., R.W.L. and R.A.H. analyzed insertion data, annotated insertions, and prepared public database submissions.

J.W.C. performed bioinformatic analysis.

K.J.T.V., N.A.H. and H.P. verified RMCE events by PCR.

K.J.T.V. and K.L.S. did stainings of gene trap events.

K.L.S. and N.A.H. did stainings of protein trap events.

K.J.T.V., K.L.S., N.A.H. and H.J.B. analyzed expression patterns.

K.J.T.V. and H.J.B. wrote the paper.

R.A.H. and R.W.L. edited the paper.

**ACCESSION NUMBERS** GenBank: GU370067 (MiMIC vector), XXX, (pBS-KS-attB1-2), XXX (pBS-KS-attB1-2-GT-SA), XXX (pBS-KS-attB1-2-PT-SA-SD-0), XXX (pBS-KS-attB1-2-PT-SA-SD-1), XXX (pBS-KS-attB1-2-PT-SA-SD-2). Genomic sequences flanking MiMIC insertion sites in the 1,269 insertion lines selected for the GDP permanent collection have been submitted to GenBank, and supporting data have been deposited in FlyBase (<http://flybase.org/>).

traps and cause mutant phenotypes to wild type by RMCE and modify insertions to control *GAL4* or *QF* overexpression systems or perform lineage analysis using the Flp system. Insertions within coding introns can be exchanged with protein-tag cassettes to create fusion proteins to follow protein expression and perform biochemical experiments. The applications of MiMIC vastly extend the *Drosophila melanogaster* toolkit.

## INTRODUCTION

Different types of transposons have been used to manipulate the *Drosophila* genome and to assess the function of genes, but each is designed for a specific purpose, and none is truly multi-faceted. The most commonly used transposons are the *P*-element, *piggyBac* and *Minos*<sup>1-3</sup>. *P*-elements mobilize efficiently and often excise imprecisely. However, they exhibit a strong insertional bias for the 5' ends of genes<sup>4, 5</sup>. *piggyBac* elements show much less bias<sup>5</sup>, but mobilize less efficiently than *P*-elements and only excise precisely<sup>6</sup>. *Minos* elements have very little insertional bias<sup>5, 7, 8</sup>, transpose stably and efficiently in numerous organisms<sup>9</sup>, and excise imprecisely at a useful frequency<sup>6, 8</sup>.

The most popular application of transposons is to create mutations directly by insertion or by imprecise excision<sup>10</sup>. Transposons have been engineered to allow controlled misexpression of genes via upstream activating sequence (*UAS*) sites in the transposon vector<sup>4, 11</sup> or to promote activation of reporters like *GAL4* or  $\beta$ -galactosidase via nearby enhancers<sup>12, 13</sup>. Transposons can also function as gene traps if they carry a splice acceptor site (*SA*) followed by stop codons in all three reading frames and a polyadenylation site so that intronic insertions can interrupt transcription and translation<sup>14</sup>. Transposons containing a protein trap harbor a *SA* followed by a coding sequence tag and a splice donor site (*SD*). When the protein trap is inserted in a coding intron in the appropriate orientation and reading frame, it reveals the protein's expression pattern<sup>15, 16</sup>. Unfortunately, the frequency of *P*-element insertions in introns is low<sup>4, 5, 17</sup>, and only 1/6th of insertions within introns have the appropriate orientation and reading frame to function as protein traps. Hence, only about 2.5% of *Drosophila* genes have been tagged with a protein trap, even when a *piggyBac* having a lesser insertional bias was used<sup>18, 19</sup>. Each different application of transposons requires the generation and maintenance of thousands of single-insertion stocks. The burden of stock keeping has limited the availability of these different tools: less than 5% of the transposon stocks that have been generated in the past 25 years are still available<sup>5</sup>. For the vast majority of *Drosophila* genes, only one type of transposon insertion is still available.

Transposons can be engineered to include target sequences recognized by recombinases or integrases<sup>3, 20, 21</sup> such as Flp<sup>22</sup> and  $\Phi$ C31<sup>23, 24</sup>, respectively. These enzymes can replace sequences within transposons via recombinase mediated cassette exchange (RMCE)<sup>25, 26</sup>. RMCE has been demonstrated in *Drosophila* with both Flp and  $\Phi$ C31<sup>27, 28</sup>.  $\Phi$ C31 integrase is the preferred enzyme due to its higher efficiency in transgenesis and unidirectional integration<sup>23, 24</sup>.

Here, we describe a new mutagenesis and genome manipulation system called *Minos* Mediated Integration Cassette (MiMIC). MiMIC is a *Minos* transposon that carries a

dominant marker and a gene trap cassette flanked by two inverted  $\Phi$ C31 *attP* sites. This transposon combines unbiased insertional mutagenesis with the ability to replace the gene trap cassette by RMCE. Using MiMIC insertions, virtually limitless gene modification and genome engineering can be performed. We illustrate the utility of this novel system through gene- and protein-trap experiments, and reversion of lethal phenotypes.

## RESULTS

### The MiMIC transposon

We engineered a new transposon vector, *Minos* Mediated Integration Cassette (MiMIC). Between the *Minos* 255-nt inverted repeats (Fig.1a), we included the *yellow*<sup>+</sup> dominant body-color marker for identifying insertions, flanked by two inverted  $\Phi$ C31 *attP* sites. We also included a mutagenic gene-trap cassette consisting of a SA followed by stop codons in all three reading frames, the coding sequence of the fluorescent protein EGFP, and an SV40 polyadenylation signal sequence. The sequences between the *attP* sites are replaceable through RMCE *in vivo* with any DNA cassette flanked by two inverted  $\Phi$ C31 *attB* sites<sup>28</sup>. This replaces the *yellow*<sup>+</sup> marker, so RMCE events can be identified by loss of body pigmentation. To demonstrate the versatility of MiMIC, we engineered three replacement cassettes: a neutral correction plasmid for removing the mutagenic gene trap in MiMIC, a gene-trap plasmid for introducing protein-coding sequences under control of the host gene promoter, and a protein-trap plasmid for incorporating reporter tags into the coding sequence of the host gene (Fig.1b and Supplementary Table 1).

Since donor cassettes can contain any DNA fragment, MiMIC provides enormous flexibility (Fig.1c). MiMIC insertions near the 5' and 3' ends of genes allow the integration of regulatory elements such as enhancers or insulators to direct or restrict expression, respectively. Such insertions can also be used to integrate an *FRT* site for creating Flp-based chromosomal rearrangements<sup>3</sup>. Insertions in 5' UTR introns allow the incorporation of binary expression components, such as *GALA/UAS*<sup>29</sup> and *QF/QUAS*<sup>30</sup> and recombinases such as Flp<sup>22</sup>. Insertions in coding introns allow integration of protein tags, including an ever-expanding repertoire of fluorescent markers and conditional protein destruction tags, and other gene-trap mutator cassettes. Finally, any insertion can be used as a generic docking site for integrating transgenes.

### A MiMIC insertion screen

We created a collection of 4,464 single-insertion MiMIC lines, determined unique insertion sites for 3,633 insertions (81.3%) by inverse PCR, and associated the mapped insertions with features of annotated genes (Online Methods). Interestingly, 2,293 (63%) of the insertions map within 1,541 annotated genes, and 72% of these intragenic insertions map within introns, including 5' UTR introns and coding introns, both of which are valuable targets for RMCE-based gene manipulation (Supplementary Table 2). We have deposited 1,269 selected insertion lines in the Bloomington *Drosophila* Stock Center (BDSC) as part of the *Drosophila* Gene Disruption Project (GDP) collection<sup>5</sup>. Additional MiMIC lines will be selected for the GDP collection on a regular basis. We aim to deposit over 6,000 lines during the next four years. The GDP maintains an online database (<http://>

[flypush.imgen.bcm.tmc.edu/pscreen/](http://flypush.imgen.bcm.tmc.edu/pscreen/)) of lines that are available from the BDSC as well as lines that are in the process of being balanced, which may be obtained directly from the GDP.

### MiMIC insertion mutants can be reverted by RMCE

The MiMIC transposon contains a gene-trap cassette. Hence, insertions in coding introns should truncate transcripts if MiMIC is inserted in the proper orientation. We selected four MiMIC transposons inserted in the proper orientation to be mutator gene traps:

*Mi{MIC}Rfx<sup>MI00053</sup>*, *Mi{MIC}tutl<sup>MI00290</sup>*, *Mi{MIC}comm<sup>MI00380</sup>*, and *Mi{MIC}wnd<sup>MI00494</sup>* inserted in *Rfx*, *tutl*, *comm* and *wnd*, respectively. All four alleles are associated with a lethal phenotype. In three cases, the insertion failed to complement previously reported mutations of these genes (Supplementary Table 3), indicating that the lethality is indeed associated with the insertion. *Mi{MIC}wnd<sup>MI00494</sup>* is the exception. However, complementation data indicate that *Mi{MIC}wnd<sup>MI00494</sup>* and the previously reported alleles<sup>31</sup> all contain second-site mutations responsible for the lethality, and that none of the transheterozygous *wnd* allelic combinations cause lethality. For *Mi{MIC}Rfx<sup>MI00053</sup>*, complementation data indicate the presence of uncoordinated escapers for all allelic combinations, a phenotype that has been previously described for *Rfx* loss-of-function mutations<sup>32</sup>.

We then removed the gene-trap cassette from *Mi{MIC}Rfx<sup>MI00053</sup>*, *Mi{MIC}tutl<sup>MI00290</sup>* and *Mi{MIC}comm<sup>MI00380</sup>* by RMCE with a correction plasmid (Fig 1b), screened for loss of *yellow<sup>+</sup>* (Supplementary Fig.1), and established that the lethality was reverted. Hence, intronic MiMIC insertions are mutagenic, and the mutation can be reverted through simple microinjection of a plasmid. This demonstrates that MiMIC is the cause of the lethal phenotypes in these three insertion alleles.

### Binary expression and lineage analysis with MiMIC

A substantial portion (20.4%) of intragenic MiMICs are localized to 5'UTR introns (Supplementary Table 2). Introduction of exogenous protein-coding sequences into these insertions allows expression under control of the endogenous gene regulatory elements. Hence, we constructed three gene-trap plasmids that encode GAL4, QF, and Flp (Fig.2a). We selected five 5'UTR intronic insertions: *Mi{MIC}gogo<sup>MI00065</sup>*, *Mi{MIC}Tl<sup>MI00181</sup>*, *Mi{MIC}caps<sup>MI00249</sup>*, *Mi{MIC}MYPT-75D<sup>MI00314</sup>* and *Mi{MIC}BM-40-SPARC<sup>MI00329</sup>*, inserted in *gogo*, *Tl*, *caps*, *MYPT-75D*, and *BM-40-SPARC*, respectively. We used RMCE to incorporate each of the three gene-trap cassettes into these insertions.

We tested the GAL4 insertions using a 10×UAS-mCherry cytoplasmic reporter (Online Methods), the QF insertions with a 5×QUAS-mtdTomato-3×HA membrane reporter<sup>30</sup>, and the Flp insertions with an act>y+>GAL4; UAS-GFP cytoplasmic Flp-out detector (Online Methods). GAL4 incorporated into the *gogo* insertion revealed expression in the embryonic peripheral and central nervous system, in agreement with RNA *in situ* hybridization data (Fig.2b,c) (Takashi Suzuki, personal communication). GAL4 inserted into *caps* faithfully recapitulated the known expression pattern<sup>33</sup> (Fig.2d,e). The unknown expression pattern of *MYPT-75D* is revealed by both GAL4, QF and Flp integrated in *Mi{MIC}MYPT-75D<sup>MI00314</sup>*. GAL4 analysis reveals numerous scattered cells labeled during

germ band extension (Fig.2f), some of which appear to be muscle precursors. This expression pattern was also revealed by QF analysis (Fig.2g), but resulted in stronger labeling due to the membrane marker driven by *QUAS* elements, instead of the cytoplasmic marker driven by *UAS* elements. Surprisingly, Flpout analysis revealed a much smaller subset of labeled cells, suggesting inefficient Flp-out (data not shown). Finally, GAL4 analysis of *BM40-SPARC* revealed an expression pattern very similar to that revealed by antibodies generated against the endogenous protein, including expression in hemocytes and fat body (Fig.2h)<sup>34, 35</sup>.

We performed PCR analysis to confirm the molecular nature of the RMCE events. In each case, PCR demonstrated that a productive binary activation or recombination activity is observed only when the cassette is integrated in the appropriate orientation for expression of the reporter (Supplementary Fig.2). Since RMCE can occur in either orientation, we expected a 50% chance of a productive exchange. However, only 25% of the gene-trap RMCE events are in the productive orientation for expression (Supplementary Table 4). Although we do not understand the cause, this suggests selection against productive reporter expression.

### Protein trapping with MiMIC insertions

To determine the expression pattern of the protein product of a gene, including its subcellular localization, one can tag with an epitope for which antibodies are available or by live imaging. More than 51% of intragenic MiMIC insertions are in coding introns and permit protein trapping (Supplementary Table 2). We constructed protein-trap cassette plasmids with SA and SD sites flanking synthetic exons encoding a series of protein tags in three versions (Fig.3a,b and Supplementary Fig.3) so as to be able to convert any MiMIC insertion in a coding intron, regardless of its orientation or splicing phase (0,1, or 2), into a protein trap. We flanked the protein tag on both sides with a linker sequence encoding a quadruple GlyGlySer repeat to increase flexibility between the tag and the host protein. We engineered seven multi-tag cassettes for different applications. Most consist of a fluorescent tag and a peptide tag so that if *in vivo* fluorescence imaging is not possible due to low expression levels, the tag can still be detected by antibodies against the tags.

In a first protein trapping test, we introduced the EGFP-FlAsH-StrepII-3×Flag multi-tag in all three phases into *Mi{MIC}CadN<sup>M100393</sup>*, which is inserted into a phase 0 intron of *CadN* (Fig.3c) and used PCR to identify integration events for each orientation and phase. As expected, only the phase 0 cassette integrated in the correct orientation recapitulated the expected expression pattern, and none of the other five classes of events resulted in detectable expression (Fig.3d).

### Protein expression analysis with multi-tag cassettes

Next, we evaluated expression patterns using seven different tags in six different genes in which MiMIC inserted in a coding intron: *Mi{MIC}Rfx<sup>M100053</sup>*, *Mi{MIC}tutl<sup>M100290</sup>*, *Mi{MIC}rhea<sup>M100296</sup>*, *Mi{MIC}comm<sup>M100380</sup>*, *Mi{MIC}CadN<sup>M100393</sup>*, and *Mi{MIC}wnd<sup>M100494</sup>*. These are inserted in *Rfx* (phase 1), *tutl* (phase 1), *rhea* (also known as *talin*) (phase 0), *comm* (phase 1), *CadN* (phase 0), and *wnd* (phase 2), respectively. We

introduced the seven different tag cassettes (Fig.3b) with the proper intron phase (Fig.3a) into each of the six insertions (Table 1). We then performed PCR analysis to determine the orientation of each RMCE event and established that 48% of the integration events are in the desired orientation. This is in agreement with the 50% frequency expected by chance, suggesting that these events are not detrimental to host gene function. Indeed, the lethality associated with each of the original gene-trap insertions was often reverted upon RMCE with protein-trap tags. For *Rfx* and *tutl*, the lethality of the MiMIC gene trap was reverted in 69% and 86% of the protein-trap lines, respectively (Table 1). This demonstrates that in most cases protein function has been at least partially restored when the gene trap is removed and replaced by a protein trap. The reverted lines may be partial loss-of-function mutations or full revertants. Note that reversion of lethality did not occur in most RMCE events for the insertions in *comm* (15%) or *wnd* (9%).

Failure to revert the lethality of a MiMIC insertion by RMCE with a protein-trap cassette may result from the effect of the tags on protein function. Alternatively, some of the MiMIC-bearing chromosomes may contain second-site lethal mutations as previously observed in *P*-element stocks exposed to transposase<sup>13</sup>, or mutations could be induced during the RMCE procedure since  $\Phi$ C31 integrase has been shown to induce DNA damage and chromosome rearrangements<sup>36–38</sup>. Both issues can be obviated by removing the second-site mutations by recombination. To test these possibilities, protein-trap alleles generated by RMCE that failed to revert the lethality of the gene-traps in *comm* (6 lines), *wnd* (4 lines), *rhea* (6 lines), and *CadN* (4 lines) were crossed to previously described alleles and deficiencies uncovering the corresponding loci. All of the protein-trap alleles of all the genes tested complemented the established lethal allele or deletion chromosome, providing evidence that the tagged fusion proteins indeed supply sufficient gene function to revert the lethality.

To determine the expression pattern and subcellular localization of the tagged proteins generated by RMCE, we first stained a large sample of tagged proteins using antibodies against GFP, V5, mCherry, and Dendra. We compared the expression of the same protein fused to different tags. Detection of *CadN* with EGFP-FIAsh-StrepII-3×Flag, EBFP2-3×Myc or Dendra-V5 shows very similar expression patterns (Fig.4a–c). Similarly, different tags integrated into *Rfx* (Fig.4d–f) and *tutl* (Fig.4g–i) show highly reproducible expression patterns. In the case of *rhea*, protein trapping allowed live imaging of three different fluorescent tags (Fig.4j–l). Furthermore, the observed expression patterns faithfully recapitulate the previously described expression patterns of *CadN*<sup>39</sup>, *Rfx*<sup>40</sup>, *tutl*<sup>41</sup> and *rhea*<sup>42</sup>. To determine in more detail whether the fusion protein expression patterns faithfully report the cellular and subcellular localization of the endogenous proteins, we performed co-labeling experiments with antibodies against different tags and the endogenous protein for *Rfx* (Fig.4m–o) and *CadN* (Fig.4p–r). These experiments showed fully overlapping expression patterns in transheterozygotes that express both the tagged and the untagged proteins.

In total, we tested 166 independent tagged fusion proteins generated by RMCE for 6 MiMIC insertions and observed that less than 3% (5/166) exhibited a different expression pattern than was anticipated. They were not associated with any particular gene or tag, suggesting



that they were due to a faulty RMCE event, and this was confirmed by an aberrant PCR pattern. These data indicate that RMCE-based protein-trapping results in the precise incorporation of tags and will permit the determination of the expression pattern and subcellular distribution of numerous uncharacterized proteins.

### Detection of new expression patterns

While analyzing the expression patterns of the different tags integrated into *Mi{MIC}wnd<sup>M100494</sup>*, we observed an expression pattern that was much broader and more complex than anticipated (Fig.4s–x and Supplementary Fig.4 online). Antibody staining<sup>31</sup> showed weak expression of Wnd in the embryonic nervous system in stage 16 embryos but not in other tissues (Fig.4u,x). However, the Wnd fusion protein generated by RMCE has a very dynamic expression pattern that is complex (Fig.4s,v) and in agreement with the pattern revealed by RNA *in situ* hybridization (Fig.4t,w). These and many other immunohistochemical staining experiments on the 166 tagged proteins (data not shown) revealed that well characterized antibodies raised against tags that are integrated in fusion proteins are often superior to custom antibodies raised against the endogenous protein.

## DISCUSSION

MiMIC permits a wide range of manipulations. Insertions in 5' UTR introns allow the expression of transcription factors such as GAL4 and QF, and recombinases such as Flp to generate gene-specific binary expression and recombination systems, respectively. Moreover, these insertions allow any current or future effector to be placed under the control of the endogenous gene's regulation. Genes that are tagged by insertions in coding introns can be manipulated in numerous ways. One can determine gene expression and subcellular protein distribution using light microscopy (Fig.4) and likely immuno-electron microscopy<sup>43</sup>. Tags inserted in transcription factors can be used for chromatin immunoprecipitation<sup>44</sup>. Other applications such as coimmunoprecipitation followed by mass spectrometry, and identification of RNA binding partners can also be performed. A complementary *in vivo* swapping approach was recently developed for enhancer trapping<sup>45</sup>.

The widespread adoption of the MiMIC system by the *Drosophila* research community will depend on substantially increasing the number of insertion lines that are available for public distribution. Currently, 1,269 unique MiMIC insertions are available from the BDSC and about 900 are being balanced and validated by re-sequencing. In the GDP, we plan to generate about 6,000 additional insertions during the next four years. Since *Minos* integrates almost at random in the genome<sup>5, 8</sup>, and about 33% of MiMIC insertions are in coding introns (Supplementary Table 2), the manipulations documented here will become feasible for many more *Drosophila* genes. The ability to assess gene expression patterns and subcellular protein distributions with high resolution (Fig.3 and 4) will vastly expand the number and quality of expression patterns of *Drosophila* genes.

Finally, both *attP* sites present in MiMIC can be used as docking sites for integration of gene targeting constructs<sup>46</sup> that can be used to engineer the genome within the vicinity of the transposon insertion. A collection of about 6,000 insertions spaced about 40 kb apart<sup>5</sup>

should allow the manipulation of most genes by engineering and integrating large genomic constructs using the P[acman] system<sup>47, 48</sup>, recombineering methods<sup>3</sup>, and RMCE<sup>28</sup>.

## ONLINE METHODS

### Molecular biology

Primers were obtained from Operon or Sigma. PCR for cloning was performed with proofreading enzymes Pfu (Stratagene) or iProof (Biorad). Bacterial colony PCR was done with Qiagen HotStarTaq DNA Polymerase (QIAGEN) or Hot MultiTaq™ DNA polymerase (US DNA). PCR purification and gel extraction were performed with the QIAquick PCR Purification and QIAquick Gel Extraction Kits (QIAGEN), respectively. Restriction enzymes and T4 DNA ligase were from NEB. The SURE or SURE2 bacterial strains (Stratagene) were used for bacterial transformation experiments. Bacteria were grown in LB broth containing 1% NaCl for plasmid isolation and ampicillin (USB) at a final concentration of 100 µg/ml. Plasmid purifications were performed using the QIAprep Spin Miniprep Kit (QIAGEN) or the PureLink™ HiPure Plasmid Kit (Invitrogen), as indicated. All cloning experiments were verified by DNA sequencing.

### Construction of the MiMIC transposon

*pMiLRTetR* was used as the *Minos* transposon backbone (gift of Stefan Oehler and Charalambos Savakis)<sup>49</sup>. *pMiLRTetR* was digested with HindIII and PacI and ligated with two annealed oligos, pMiLR-Correction-TOP and pMiLR-Correction-BOTTOM (Supplementary Table 5 for all primer sequences), resulting in the mini *Minos* plasmid, *pMiLR-Correction*.

Next, two 100-bp *attP* sites were obtained by PCR from pTA-attP (gift of Michelle Calos)<sup>50</sup>, the first one amplified with primers attP1-pMiLR-F and attP1-pMiLR-R, the second one amplified with primers attP2-pMiLR-F and attP2-pMiLR-R. Both *attP* amplicons, the first cut with HindIII and XhoI, and the second cut with XhoI and SacII, were ligated together into *pMiLR-Correction* cut with HindIII and SacII, resulting in the mini-*Minos*-attP plasmid, *pMiLR-attP1-2*. This plasmid has a stuffer fragment between each *attP* site and *Minos* inverted repeat that allows a specific inverse PCR reaction at either end (see below), as well as a multiple cloning site between the two inverted *attP* sites.

Subsequently, the intronless dominant body color marker *yellow*<sup>+</sup> (*y*[+mDint2]) obtained from EPgy2<sup>4</sup> was subcloned as a Sall fragment into the MCS of *pMiLR-attP1-2*, resulting in *pMiLR-attP1-2-yellow*.

Finally, a gene-trap cassette was constructed, consisting of the *Mhc* intron 18 SA site<sup>51</sup> obtained from *pP-GC* (gift of Xavier Morin and William Chia)<sup>15</sup> and amplified with primers MHC-SA-XmaI-F and MHC-SA-EGFP-R, and an EGFP with SV40 polyadenylation signal obtained from *pCA-GAP-Mut4-EGFP* (gift of Ami Okada)<sup>52</sup> and amplified with primers MHC-SA-EGFP-F and EGFP-SpeI-R. The two fragments were fused together using hybrid PCR<sup>53</sup> and subcloned as an XmaI-SpeI fragment into *pMiLR-attP1-2-yellow*, resulting in the final transposon plasmid *pMiLR-attP1-2-yellow-SA-EGFP*, abbreviated to MiMIC or Mi{MIC}.



## Generation of single-insertion MiMIC lines

Initial MiMIC transposition experiments were performed by co-injection of the MiMIC plasmid purified using the PureLink™ HiPure Plasmid Kit (Invitrogen) and mRNA encoding the *Minos* transposase generated from *pBlueSKMimRNA* (gift of Anastasios Pavlopoulos)<sup>54</sup> by *in vitro* transcription after NotI linearization using the mMessage mMachinE T7 Kit (Ambion) as described<sup>47, 54</sup>. Co-injection titration experiments were performed with plasmid/transposase concentrations (ng/μl) of 300/300, 300/100, 100/300 and 100/100. Injections were performed into a  $y^* w^*$  strain. Transgenic lines were mapped by genetic crosses using  $y^* w^*$ ;  $T(2;3)ap^{Xa}/SM5;TM3, Sb$  and balanced with  $P\{w[+mW.Scer\backslash FRT.hs]=RS3\}l(1)CB-6411-3^1, w^{1118}/FM7h$  (BL6878) for the X chromosome,  $y^1 w^{67c23}$ ;  $In(2LR)Gla, wg^{Gla-1}/SM6a$  (BL6600) for chromosome 2,  $y^* w^*$ ;  $D/TM6b, Hu, Tb$  (Bellen lab) for chromosome 3 or  $y^*$ ;  $ry^{506/+}$ ;  $Ci^D/ey^D$  for chromosome 4 (Bellen lab).

Subsequently, five MiMIC insertions on the X chromosome (Mi{MIC}MI00019, Mi{MIC}MI00030, Mi{MIC}MI00039, Mi{MIC}MI00040 and *Mi{MIC}MI00069*), obtained from the co-injection experiments, were remobilized to the autosomes using a transgenic source of transposase under the control of a heat-shock promoter ( $P\{hsILMiT\}$ , FlyBase ID FBtp0021508) inserted on a second chromosome balancer ( $P\{hsILMiT\}2.4$ ; FlyBase ID FBti0073645) (gift of Charalambos Savakis)<sup>8</sup>. To allow the identification of new MiMIC remobilization events by screening for  $y^+$ , this transposase source was moved into a  $y w$  background with  $y^1 w^*$ ;  $nub^2 b^1 noc^{Sco} pr^1 cn^1/CyO$  (BL3628) resulting in  $y w$ ;  $nub^2 b^1 noc^{Sco} pr^1 cn^1/SM6a, P\{hsILMiT\}2.4$ . Heat shocks were performed for 2 hours in a 37° water bath on 5 consecutive days. Transposition efficiencies were initially as high as 43% for *Mi{MIC}MI00040*, but eventually dropped to about 7% for all donor insertions tested, for unknown reasons. Insertions in males were balanced with  $y^* w^*$ ;  $T(2;3)ap^{Xa}/SM5;TM3, Sb$ . Insertions on the 4<sup>th</sup> chromosome were balanced with  $y^*$ ;  $ry^{506/+}$ ;  $ci^D/ey^D$  as described above.

During a second phase, three MiMIC insertions on the X chromosome (*Mi{MIC}MI00019*, *Mi{MIC}MI00030*, and *Mi{MIC}MI00040*) were remobilized to the  $TM3, Sb$  balancer chromosome, resulting in two independent 3<sup>rd</sup> chromosome transposon-donor balancer chromosomes, which we named MI00000A and MI00000B. These donor chromosomes were used to remobilize MiMIC to the X chromosome and autosomes using the  $y w$ ;  $noc^{Sco} nub^2 b^1 noc^{Sco} pr^1 cn^1/SM6a, P\{hsILMiT\}2.4$  stock described above. In addition *Mi{MIC}MI00827* located on the X chromosome was mobilized to the autosomes.

## Mapping and annotation of MiMIC insertion sites

We generated 4,464 strains containing insertions of the MiMIC transposon (nearly always single insertions) and mapped 3,633 insertions to a unique site in the reference genome sequence (Release 5; <http://www.fruitfly.org>). Sequences flanking MiMIC insertions were determined by inverse PCR and DNA sequencing, and mapped by alignment to the genome sequence, as described for MB lines in<sup>5</sup> with one modification: genomic DNA was digested with Sau3A I or MboI (which are isoschizomers). A detailed protocol is available on the GDP website (<http://flypush.imgen.bcm.tmc.edu/pscreen/>). Lines that were selected for the

GDP collection were balanced, and their insertion sites verified by re-sequencing before delivery to the BDSC.

We associated MiMIC insertions with annotated genes and gene features (FlyBase r5.32). Annotated features of one gene transcript often overlap those of another transcript, so we adopted a progressive strategy for associating MiMIC insertions with gene features, such that each insertion was assigned to only one feature. We first associated insertions with coding exons, followed by 5' UTR exons, 3' UTR exons, coding introns, 5' UTR introns, and 3' UTR introns. The remaining insertions were classified as intergenic. Note that this is a conservative approach that underestimates the number of insertions associated with lower ranked gene features.

### Construction of correction cassettes for RMCE

Two 100-bp fragments containing *attB* sites were obtained by PCR from *pTA-attB* (gift of Michelle Calos)<sup>50</sup>, the first amplified with primers attB1-pBS-F and attB1-pBS-R, and the second amplified with primers attB2-pBS-F and attB2-pBS-R. The *attB* amplicons, the first cut with SacI and EcoRI, and the second cut with EcoRI and KpnI, were ligated together into *pBS-KS* and *pBS-SK* cut with SacI and KpnI, resulting in the mini-*attB*-RMCE plasmids, *pBS-KS-attB1-2* and *pBS-SK-attB1-2*. These plasmids have two inverted *attB* sites flanking a multiple cloning site (XbaI, SpeI, PstI, EcoRI, XhoI, BamHI and HindIII).

### Construction of gene-trap cassettes for RMCE

A gene-trap cassette incorporating the *Mhc* intron 18 SA site<sup>51</sup> was PCR amplified from *pP-GC* (gift of Xavier Morin and William Chia)<sup>15</sup> with primers SA-XbaI-F and SA-PstI-R. The resulting PCR fragment was cut with XbaI and PstI and subcloned into *pBS-KS-attB1-2*, cut with XbaI and PstI, resulting in the mini gene-trap plasmid, *pBS-KS-attB1-2-GT-SA*. The SA is followed by a multiple cloning site (PstI, EcoRI, XhoI, BamHI and HindIII).

A mutagenic GAL4 gene-trap cassette, encompassing the GAL4 coding sequence and *Hsp70* polyadenylation signal, was obtained from plasmid *pChs-GAL4* (Drosophila Genomics Resource Center)<sup>55</sup>, and PCR amplified with primers GAL4-Hsp70-EcoRI-F and GAL4-Hsp70-BamHI-R. A mutagenic QF gene-trap cassette, encompassing the QF coding sequence and *Hsp70* polyadenylation signal, was obtained from plasmid *pattB-QF-Hsp70* (Addgene)<sup>30</sup>, and PCR amplified with primers QF-SV40-EcoRI-F and QF-SV40-BamHI-R. A mutagenic Flp fate mapping gene-trap cassette, encompassing the FLPo<sup>56</sup> coding sequence and SV40 polyadenylation signal, was obtained from plasmid *pQUAS-DSCP-Flpo* (Addgene)<sup>30</sup>, and PCR amplified with primers Flpo-SV40-EcoRI-F and Flpo-SV40-BamHI-R. The resulting PCR fragments were cut with EcoRI and BamHI and subcloned into *pBS-KS-attB1-2-GT-SA*, cut with EcoRI and BamHI, resulting in the plasmids *pBS-KS-attB1-2-GT-SA-GAL4-Hsp70*, *pBS-KS-attB1-2-GT-SA-Flp-SV40*, and *pBS-KS-attB1-2-GT-SA-QF-Hsp70* respectively.

### Construction of protein-trap cassettes for RMCE

Protein-trap cassettes were constructed for the three intron phases (0, 1, 2). The *Mhc* intron 18 SA and intron 17 SD sites<sup>51</sup> were obtained from *pP-GC* (gift of Xavier Morin and

William Chia)<sup>15</sup>. The protein trap with splice phase 0 was generated from two PCR fragments, the SA site amplified with primers SA-XbaI-F and SA-SD-Phase-0-R, and the SD site amplified with primers SA-SD-Phase-0-F and SD-HindIII-R. The protein trap with splice phase 1 was generated from two PCR fragments, the SA site amplified with primers SA-XbaI-F and SA-SD-Phase-1-R, and the SD site amplified with primers SA-SD-Phase-1-F and SD-HindIII-R. The protein trap with splice phase 2 was generated from two PCR fragments, the SA site amplified with primers SA-XbaI-F and SA-SD-Phase-2-R, and the SD site amplified with primers SA-SD-Phase-2-F and SD-HindIII-R. For each intron phase construct, the SA PCR fragment was cut with XbaI and BamHI, the SD PCR fragment was cut with BamHI and HindIII, and the digested fragments were subcloned in a three-way ligation into *pBS-KS-attB1-2*, cut with XbaI and HindIII, resulting in *pBS-KS-attB1-2-PT-SA-SD-0*, *pBS-KS-attB1-2-PT-SA-SD-1* and *pBS-KS-attB1-2-PT-SA-SD-2*. These plasmids contain the SA site, a phase linker for phase 0, 1 or 2, and the SD site, between two inverted *attB* sites. The phase linker consists of a BamHI site used to subclone protein-trap tags (see below) between two (GlyGlySer)<sub>4</sub> peptide-encoding linkers that may provide flexibility between the protein trap tag and the endogenous protein sequences (see below) (Supplementary Figure 3).

The fluorescent protein tag mCherry (gift of Roger Tsien)<sup>57</sup> was used without codon optimization. The following protein and peptide tags were generated by gene synthesis by GENEART (<http://www.geneart.com/>) with codon usage biased toward *Drosophila melanogaster*: superfolder GFP<sup>58</sup>, enhanced blue fluorescent protein 2<sup>59</sup>, TagRFP-T<sup>60</sup>, HRP<sup>61</sup>, Dendra2<sup>62, 63</sup>, KillerRed<sup>64</sup>, optimized FAsH peptide<sup>65</sup>, StrepII peptide<sup>66</sup>, 3×Flag peptide<sup>67</sup>, 3×Myc peptide<sup>68</sup>, 3×HA peptide<sup>69</sup> and the TEV protease site<sup>70</sup>. The following peptide tags were generated by PCR and primer addition with codon usage biased towards *Drosophila melanogaster* based on the Codon Usage Database (<http://www.kazusa.or.jp/codon/>): S peptide<sup>71</sup> and V5 peptide<sup>72</sup>. The following multi-itags were generated through hybrid PCR<sup>53</sup> or PCR and primer addition, and subcloned in customized vector backbones (KJTV, unpublished): EGFP-FAsH-StrepII-TEV-3×Flag, EBFP2-3×Myc, TagRFP-T-3×HA, HRP-S, Dendra-V5, KillerRed-V5.

The tags were then amplified by PCR as BamHI-Insert-GGC-BamHI fragments, to correct for cloning and reconstitution of the (GlyGlySer)<sub>4</sub> linker (Supplementary Figure 3), and subcloned into the three-phase protein-trap plasmids described above. PCR amplification of EGFP-FAsH-StrepII-TEV-3×Flag was performed with primers EGFPmultiFINAL-F and EGFPmultiFINAL-R, resulting in *pBS-KS-attB1-2-PT-SA-SD-0-EGFP-FAsH-StrepII-TEV-3×Flag*, *pBS-KS-attB1-2-PT-SA-SD-1-EGFP-FAsH-StrepII-TEV-3×Flag* and *pBS-KS-attB1-2-PT-SA-SD-2-EGFP-FAsH-StrepII-TEV-3×Flag*. PCR amplification of mCherry was performed with primers Cherry-F and Cherry-R, resulting in *pBS-KS-attB1-2-PT-SA-SD-0-mCherry*, *pBS-KS-attB1-2-PT-SA-SD-1-mCherry* and *pBS-KS-attB1-2-PT-SA-SD-2-mCherry*. PCR amplification of EBFP2-3×Myc was performed with primers EBFP2-Myc-F and EBFP2-Myc-R resulting in *pBS-KS-attB1-2-PT-SA-SD-0-EGFP-EBFP2-3×Myc*, *pBS-KS-attB1-2-PT-SA-SD-1-EBFP2-3×Myc* and *pBS-KS-attB1-2-PT-SA-SD-2-EBFP2-3×Myc*. PCR amplification of TagRFP-T-3×HA was performed with primers TagRFP-HA-F and TagRFP-HA-R, resulting in *pBS-KS-attB1-2-PT-SA-SD-0-TagRFP-*

*T-3×HA*, *pBS-KS-attB1-2-PT-SA-SD-1-TagRFP-T-3×HA* and *pBS-KS-attB1-2-PT-SA-SD-2-TagRFP-T-3×HA*. PCR of HRP-S was performed with primers HRP-S-F, HRP-S-R1 and HRP-S-R2, resulting in *pBS-KS-attB1-2-PT-SA-SD-0-HRP-S*, *pBS-KS-attB1-2-PT-SA-SD-1-HRP-S* and *pBS-KS-attB1-2-PT-SA-SD-2-HRPS*. PCR of Dendra-V5 was performed with primers Dendra-V5-F, Dendra-V5-R1 and Dendra-V5-R2, resulting in *pBS-KS-attB1-2-PT-SA-SD-0-Dendra-V5*, *pBS-KS-attB1-2-PT-SA-SD-1-Dendra-V5* and *pBS-KS-attB1-2-PT-SA-SD-2-Dendra-V5*. PCR of KillerRed-V5 was performed with primers KillerRed-V5-F, KillerRed-V5-R1 and KillerRed-V5-R2 resulting in *pBS-KS-attB1-2-PT-SA-SD-0-KillerRed-V5*, *pBS-KS-attB1-2-PT-SA-SD-1-KillerRed-V5* and *pBS-KS-attB1-2-PT-SA-SD-2-KillerRed-V5*.

### ΦC31-mediated RMCE

Initial RMCE tests were performed with *pBS-KS-attB1-2* to ensure functionality of the plasmid backbone, since this plasmid is the progenitor of all constructs for protein-trap cassettes and other cassettes. *pBS-KS-attB1-2* DNA was purified and co-injected with ΦC31 integrase mRNA, obtained from *pET11ΦC31pA* (a gift from Michelle Calos)<sup>23</sup> by *in vitro* transcription after *Bam*HI linearization using the mMessage mMachine T7 Kit (Ambion) as described<sup>23, 47</sup>. Microinjections were performed using the RMCE landing site 25C (gift of Jack Bateman and Ting Wu)<sup>28</sup> at a plasmid concentration of 123 ng/μl and an mRNA concentration of 600 ng/μl. A transgenesis efficiency of 17.5% was obtained.

Subsequent injections were performed with transgenic ΦC31 integrase sources driven by *vasa* promoter elements located on the X chromosome (*y<sup>1</sup>M{vas-int.B}ZH-2A w\**) or the 4<sup>th</sup> chromosome (*y<sup>1</sup>w\**; *M{vas-int.B}ZH-102D*) (gifts of Johannes Bischof, Francois Karch and Konrad Basler)<sup>24</sup>. Plasmid was generally diluted to a concentration between 30 and 100 ng/μl. Microinjections were performed using the following MiMIC insertion lines: *Mi{MIC}tutl<sup>MI00290</sup>* and *Mi{MIC}CadN<sup>MI00393</sup>* on chromosome 2, and *Mi{MIC}Rfx<sup>MI00053</sup>*, *Mi{MIC}gogo<sup>MI00065</sup>*, *Mi{MIC}Tl<sup>MI00181</sup>*, *Mi{MIC}caps<sup>MI00249</sup>*, *Mi{MIC}rhea<sup>MI00296</sup>*, *Mi{MIC}MYPT-75D<sup>MI00314</sup>*, *Mi{MIC}BM-40-SPARC<sup>MI00329</sup>*, *Mi{MIC}comm<sup>MI00380</sup>*, and *Mi{MIC}wnd<sup>MI00494</sup>* on chromosome 3. When lines contained a gene-trap insertion, they were injected as heterozygous balanced stocks. Microinjections were performed by crossing males from appropriate MiMIC lines to virgin females containing the ΦC31 integrase source. Since RMCE results in a genetically unmarked chromosome due to the removal of the *y[+mDint2]* marker, fly stocks were generated that contained the ΦC31 integrase source in a balanced background for the 2<sup>nd</sup> or 3<sup>rd</sup> chromosome to maintain the MiMIC insertion balanced in G<sub>0</sub> animals: *y<sup>1</sup>M{vas-int.B}ZH-2A w\**; *noc<sup>Sco</sup>/CyO* and *y<sup>1</sup>M{vas-int.B}ZH-2A w\**; *Sb/TM6b*, *Hu*, *Tb*. Appropriate G<sub>0</sub> animals were crossed to balancer virgins: *y<sup>1</sup>w<sup>67c23</sup>*; *In(2LR)Gla*, *wg<sup>Gla-1</sup>/SM6a* (BL6600) for chromosome 2 RMCE experiments, or *y\* w\**; *D/TM6b*, *Hu*, *Tb* for chromosome 3 RMCE experiments. Transgenic G<sub>1</sub> flies were scored for the absence of a yellow<sup>+</sup> phenotype (loss of the *y[+mDint2]* marker) over a balancer or dominantly marked chromosome appropriate for the chromosome, and crossed to balancer virgins: *y<sup>1</sup>w<sup>67c23</sup>*; *In(2LR)Gla*, *wg<sup>Gla-1</sup>/SM6a* (BL6600) (chromosome 2), or *y\* w\**; *D/TM6b*, *Hu*, *Tb* (chromosome 3). Balanced transgenic G<sub>2</sub> flies were intercrossed to establish stocks. A list with all RMCE efficiencies is available in Supplementary Table 6.

## Molecular characterization of integration events

For PCR verification of RMCE integration events, DNA was extracted from 10 to 15 adult flies using the PureLink™ Genomic DNA Mini Kit (Invitrogen). PCR was performed with tag-specific primers and MiMIC specific primers. Tag-specific primers (Tag-F and Tag-R) are mCherry-Seq-F and mCherry-Seq-R for mCherry, EGFPdo-Seq-F and EGFPdo-Seq-R for EGFP, EBFP2do-Seq-F and EBFP2do-Seq-R for EBFP2, TagRFPdo-Seq-F and TagRFPdo-Seq-R for TagRFP, Hrpdo-Seq-F and Hrpdo-Seq-R for HRP, Dendrado-Seq-F and Dendrado-Seq-R for Dendra, Killerreddo-Seq-F and Killerreddo-Seq-R for Killerred, GAL4-1R and GAL4-5F for GAL4, FLP0-Seq-R and SV40pA-Long-F for Flpo, and QF-Seq-R1 and Hsp70-pA-Alt-F for QF. MiMIC specific primers are Orientation-MiL-F and Orientation-MiL-R. PCR reaction conditions were: 1 µl DNA, 1 µl primer 1, 1 µl primer 2, 2 µl 10× Buffer, 0.16 µl dNTPs (25 mM each), 0.08 µl Qiagen HotStarTaq DNA Polymerase (QIAGEN), 14.76 µl milliQ water. PCR cycling conditions in PTC-225 or DNA Engine (MJ Research) were: denaturation at 94° for 10 minutes, 40 cycles at 94° for 30 seconds, 60° for 30 seconds and 72° for 60 seconds, and post-amplification extension at 72° for 10 minutes.

For each RMCE event, 4 PCR reactions were performed: a first PCR reaction with primers Orientation-MiL-F and Tag-R, a second PCR reaction with primers Orientation-MiL-F and Tag-F, a third PCR reaction with primers Orientation-MiL-R and Tag-R, and a fourth PCR reaction with primers Orientation-MiL-R and Tag-F. Since the transposon integrates one or two orientations relative to the gene, only one in two RMCE events is productive with respect to creating a gene trap or protein trap, which is reflected in a positive PCR for reactions 1 and 4, or 2 and 3. A “1/4” PCR pattern is always desired for a productive RMCE event (for example a gene or protein trap), when the gene/transposon configuration is 1/1 or -1/-1. Conversely, a “2/3” PCR pattern is diagnostic of a productive RMCE event, when the gene/transposon configuration is 1/-1 or -1/1. The reverse holds for unproductive RMCE events (Supplementary Figure 2).

## Genetic complementation testing

Genetic complementation tests were performed between lethal MiMIC insertion lines, or lethal RMCE derivatives of both lethal and viable MiMIC lines, and previously described mutant alleles. *Mi{MIC}Rfx<sup>M100053</sup>* was tested with *Rfx<sup>49</sup>* and *Rfx<sup>253</sup>* (gifts of Anne Laurençon and Benedicte Durand)<sup>32</sup>, and *Df(3R)Exel6157* (BL7636)<sup>73</sup>. *Mi{MIC}tutl<sup>M100290</sup>* was tested with *P{ry<sup>+17.2</sup>=PZ}tutl<sup>01085</sup>* (Bloomington stock number BL10979), *tutl<sup>4</sup>* (gift of Kendal Broadie)<sup>41</sup>, *tutl<sup>23</sup>* and *tutl<sup>GAL4</sup>* (gifts of Yong Rao)<sup>74</sup>, *tutl<sup>ex383</sup>* (gift of Bader Al-Anzi)<sup>75</sup> and *Df(2L)ed-dp* (BL702). *Mi{MIC}rhea<sup>M100296</sup>* was tested with *rhea<sup>1</sup>* (BL2296) and *Df(3L)W10* (BL2608). *Mi{MIC}comm<sup>M100380</sup>* was tested with *comm<sup>A490</sup>* and *comm<sup>e39</sup>* (gifts of Guy Tear)<sup>76</sup>, and *P{w<sup>+mCy+mDint2</sup>=EPgy2}comm<sup>EY10154</sup>* (BL17644), *Df(3L)BK10* (BL2992) and *Df(3L)fz-M21* (BL5461). *Mi{MIC}CadN<sup>M100393</sup>* was tested with *CadN<sup>M19FRT40A</sup>* and *CadN<sup>18A FRT40A</sup>* (gifts of Larry Zipursky)<sup>39, 77</sup>, and *Df(2L)Exel7069* (BL7837). *Mi{MIC}wnd<sup>M100494</sup>* was tested with *wnd<sup>1</sup>*, *wnd<sup>2</sup>* and *wnd<sup>3</sup>* (gifts of Aaron DiAntonio)<sup>31</sup>, and *Df(3L)XS705* (BL5584) and *Df(3L)Exel9007* (BL7942). Complementation tests for lethal protein-trap events were performed similarly.



## GAL4/UAS, QF/QUAS and Flp experiments

RMCE experiments using the binary expression factors GAL4 and QF, and the Flp recombinase system were tested as follow: GAL4 swaps were crossed to  $y\ w$ ; *VK19: .10×UAS-mCherry-SV40* which provides strong mCherry overexpression driven by 10×UAS in a customized P[acman] construct (KJTV, unpublished), and were analyzed as described below. QF swaps were crossed to  $y^1w^{1118}; P\{w^{+mC}=QUAS-mtdTomato-3\times HA\}26$  (BL30005)<sup>30</sup> and analyzed as described below. Flp swaps were crossed to a customized actin-GAL4-Flp-out line driving UAS-EGFP (H.J.B., unpublished) and analyzed as described below.

## Expression analysis

The following antibodies were used for expression analysis: mouse anti-CadN (DN-Ex#8) at 1:200<sup>39</sup> (Developmental Studies Hybridoma Bank), rabbit anti-RFX at 1:5000 (a gift from Anne Laurençon and Benedicte Durand)<sup>40</sup>, rabbit anti-Wnd at 1:500 (a gift from Aaron DiAntonio)<sup>31</sup>, rabbit anti-GFP at 1:250 (Invitrogen), mouse anti-DsRed at 1:250 (Clontech), rabbit anti-TagRFP at 1:500 (Evrogen), rabbit anti-Dendra2 at 1:5000 (Evrogen), rabbit anti-Killerred at 1:1000 (Evrogen), mouse anti-Flag at 1:250 (Sigma-Aldrich), mouse anti-StrepII at 1:200 (Thermo Scientific), mouse anti-S at 1:100 (Thermo Scientific), mouse anti-V5 at 1:2000 (Invitrogen), mouse anti-c-Myc at 1:250 (Abcam) and mouse anti-HA at 1:200 (Covance).

*Drosophila* embryos (0 to 24 hours) were collected on grape-agar plates and were subsequently fixed for 20 minutes in a 1:1 mixture of 0.38% formaldehyde in PBS and heptane. The fixative was then removed and methanol added. After vigorously shaking, the heptane-methanol mixture was replaced by methanol, whereupon methanol was replaced by ethanol. Upon rehydration in PBS/0.2% Triton, embryos were blocked for 1 hour in PBS, 10% normal goat serum and incubated overnight with primary antibodies. Fluorescently labeled or HRP-conjugated secondary antibodies were obtained from Jackson ImmunoResearch and were used at a 1:250 dilution.

## mRNA *in situ* hybridization

A 1 kb PCR fragment was obtained with primers Wnd-F and Wnd-R from the Wnd cDNA clone LD14856<sup>78</sup> and subcloned into the *pGemTeasy* vector (Promega). *In vitro* transcription was performed according to standard procedures, using the DIG RNA labeling kit (Roche). Fixation and *in situ* hybridization were carried out following the Krause protocol<sup>79</sup>. The digoxigenin labeled RNA probes were detected by alkaline phosphatase reaction, using the Lehmann protocol<sup>80</sup>.

## Supplementary Material

Refer to Web version on PubMed Central for supplementary material.

## ACKNOWLEDGEMENTS

We thank B. Al-Anzi (Caltech), Konrad Basler (University of Zurich), J. Bateman (Bowdoin College), J. Bischof (University of Zurich), K. Broadie (Vanderbilt University), M. Calos (Stanford University), W. Chia (National



University of Singapore), A. DiAntonio (Washington University), B. Durand (University of Lyon), F. Karch (University of Geneva), A. Laurençon (University of Lyon), L. Luo (Stanford University), X. Morin (Institute of Developmental Biology of Marseille), A. Nose (University of Tokyo), S. Oehler (University of Crete), A. Okada (Stanford University), A. Pavlopoulos (University of Cambridge), C. Potter (Johns Hopkins University), Y. Rao (McGill University), M. Ringuette (University of Toronto), C. Savakis (Biomedical Sciences Research Center Alexander Fleming), J. Shahab (University of Toronto), T. Suzuki (Max Planck Institute of Neurobiology), C. Tan (University of Missouri), G. Tear (King's College London), R. Tsien (University of California San Diego), T. Wu (Harvard University), L. Zipursky (University of California Los Angeles), the Bloomington *Drosophila* Stock Center (Indiana University), the *Drosophila* Genomics Resource Center (Indiana University), Addgene, and the Developmental Studies Hybridoma Bank for flies, plasmids, antibodies and communications. We thank S. Park and K. Wan at LBNL for assistance in mapping MiMIC insertions. We especially thank D. Bei, Y. Fang, J. Li, Z. Wang, X. Zheng and J. Yue for generating fly stocks. We thank T. Suzuki (Max Planck Institute of Neurobiology) for communication of unpublished results. This work was funded by NIH grant 2R01 GM067858 to A.C.S., R.A.H. and H.J.B. A.C.S. and H.J.B. are Investigators of the Howard Hughes Medical Institute. Plasmids are available through the *Drosophila* Genomics Resource Center (<https://dgrc.cgb.indiana.edu/vectors/>). Fly strains are available through the Bloomington *Drosophila* Stock Center.

## REFERENCES

- Ryder E, Russell S. Transposable elements as tools for genomics and genetics in *Drosophila*. *Brief. Funct. Genomic. Proteomic.* 2003; 2:57–71. [PubMed: 15239944]
- Venken KJ, Bellen HJ. Emerging technologies for gene manipulation in *Drosophila melanogaster*. *Nat. Rev. Genet.* 2005; 6:167–178. [PubMed: 15738961]
- Venken KJ, Bellen HJ. Transgenesis upgrades for *Drosophila melanogaster*. *Development.* 2007; 134:3571–3584. [PubMed: 17905790]
- Bellen HJ, et al. The BDGP gene disruption project: single transposon insertions associated with 40% of *Drosophila* genes. *Genetics.* 2004; 167:761–781. [PubMed: 15238527]
- Bellen, HJ., et al. The *Drosophila* Gene Disruption Project: Progress Using Transposons With Distinctive Site-Specificities. 2011. in press
- Witsell A, Kane DP, Rubin S, McVey M. Removal of the bloom syndrome DNA helicase extends the utility of imprecise transposon excision for making null mutations in *Drosophila*. *Genetics.* 2009; 183:1187–1193. [PubMed: 19687136]
- Franz G, Savakis C. Minos, a new transposable element from *Drosophila hydei*, is a member of the Tc1-like family of transposons. *Nucleic Acids Res.* 1991; 19:6646. [PubMed: 1661410]
- Metaxakis A, Oehler S, Klinakis A, Savakis C. Minos as a genetic and genomic tool in *Drosophila melanogaster*. *Genetics.* 2005; 171:571–581. [PubMed: 15972463]
- Pavlopoulos A, Oehler S, Kapetanaki MG, Savakis C. The DNA transposon Minos as a tool for transgenesis and functional genomic analysis in vertebrates and invertebrates. *Genome Biol.* 2007; 8(Suppl 1):S2. [PubMed: 18047694]
- Spradling AC, et al. The Berkeley *Drosophila* Genome Project gene disruption project: Single P-element insertions mutating 25% of vital *Drosophila* genes. *Genetics.* 1999; 153:135–177. [PubMed: 10471706]
- Rorth P, et al. Systematic gain-of-function genetics in *Drosophila*. *Development.* 1998; 125:1049–1057. [PubMed: 9463351]
- Bier E, et al. Searching for pattern and mutation in the *Drosophila* genome with a P-lacZ vector. *Genes Dev.* 1989; 3:1273–1287. [PubMed: 2558049]
- Bellen HJ, et al. P-element-mediated enhancer detection: a versatile method to study development in *Drosophila*. *Genes Dev.* 1989; 3:1288–1300. [PubMed: 2558050]
- Lukacsovich T, et al. Dual-tagging gene trap of novel genes in *Drosophila melanogaster*. *Genetics.* 2001; 157:727–742. [PubMed: 11156992]
- Morin X, Daneman R, Zavortink M, Chia W. A protein trap strategy to detect GFP-tagged proteins expressed from their endogenous loci in *Drosophila*. *Proc. Natl. Acad. Sci. U. S. A.* 2001; 98:15050–15055. [PubMed: 11742088]
- Clyne PJ, Brotman JS, Sweeney ST, Davis G. Green fluorescent protein tagging *Drosophila* proteins at their native genomic loci with small P elements. *Genetics.* 2003; 165:1433–1441. [PubMed: 14668392]

17. Aleksic J, Lazic R, Muller I, Russell SR, Adryan B. Biases in *Drosophila melanogaster* protein trap screens. *BMC. Genomics*. 2009; 10:249. [PubMed: 19476619]
18. Quinones-Coello AT, et al. Exploring strategies for protein trapping in *Drosophila*. *Genetics*. 2007; 175:1089–1104. [PubMed: 17179094]
19. Buszczak M, et al. The carnegie protein trap library: a versatile tool for *Drosophila* developmental studies. *Genetics*. 2007; 175:1505–1531. [PubMed: 17194782]
20. Branda CS, Dymecki SM. Talking about a revolution: The impact of site-specific recombinases on genetic analyses in mice. *Dev. Cell*. 2004; 6:7–28. [PubMed: 14723844]
21. Wirth D, et al. Road to precision: recombinase-based targeting technologies for genome engineering. *Curr. Opin. Biotechnol*. 2007; 18:411–419. [PubMed: 17904350]
22. Golic KG, Lindquist S. The FLP recombinase of yeast catalyzes site-specific recombination in the *Drosophila* genome. *Cell*. 1989; 59:499–509. [PubMed: 2509077]
23. Groth AC, Fish M, Nusse R, Calos MP. Construction of transgenic *Drosophila* by using the site-specific integrase from phage  $\phi$ C31. *Genetics*. 2004; 166:1775–1782. [PubMed: 15126397]
24. Bischof J, Maeda RK, Hediger M, Karch F, Basler K. An optimized transgenesis system for *Drosophila* using germ-line-specific  $\phi$ C31 integrases. *Proc. Natl. Acad. Sci. U. S. A.* 2007; 104:3312–3317. [PubMed: 17360644]
25. Schlake T, Bode J. Use of mutated FLP recognition target (FRT) sites for the exchange of expression cassettes at defined chromosomal loci. *Biochemistry*. 1994; 33:12746–12751. [PubMed: 7947678]
26. Baer A, Bode J. Coping with kinetic and thermodynamic barriers: RMCE, an efficient strategy for the targeted integration of transgenes. *Curr. Opin. Biotechnol*. 2001; 12:473–480. [PubMed: 11604323]
27. Horn C, Handler AM. Site-specific genomic targeting in *Drosophila*. *Proc. Natl. Acad. Sci. U. S. A.* 2005; 102:12483–12488. [PubMed: 16116081]
28. Bateman JR, Lee AM, Wu CT. Site-Specific Transformation of *Drosophila* via  $\phi$ C31 Integrase-Mediated Cassette Exchange. *Genetics*. 2006; 173:769–777. [PubMed: 16547094]
29. Brand AH, Perrimon N. Targeted gene expression as a means of altering cell fates and generating dominant phenotypes. *Development*. 1993; 118:401–415. [PubMed: 8223268]
30. Potter CJ, Tasic B, Russler EV, Liang L, Luo L. The Q system: a repressible binary system for transgene expression, lineage tracing, and mosaic analysis. *Cell*. 2010; 141:536–548. [PubMed: 20434990]
31. Collins CA, Wairkar YP, Johnson SL, Diantonio A. Highwire restrains synaptic growth by attenuating a MAP kinase signal. *Neuron*. 2006; 51:57–69. [PubMed: 16815332]
32. Dubruille R, et al. *Drosophila* regulatory factor X is necessary for ciliated sensory neuron differentiation. *Development*. 2002; 129:5487–5498. [PubMed: 12403718]
33. Shishido E, Takeichi M, Nose A. *Drosophila* synapse formation: regulation by transmembrane protein with Leu-rich repeats, CAPRICIOUS. *Science*. 1998; 280:2118–2121. [PubMed: 9641918]
34. Martinek N, Zou R, Berg M, Sodek J, Ringuette M. Evolutionary conservation and association of SPARC with the basal lamina in *Drosophila*. *Dev. Genes Evol*. 2002; 212:124–133. [PubMed: 11976950]
35. Martinek N, Shahab J, Saathoff M, Ringuette M. Haemocyte-derived SPARC is required for collagen-IV-dependent stability of basal laminae in *Drosophila* embryos. *J. Cell Sci*. 2008; 121:1671–1680. [PubMed: 18445681]
36. Ehrhardt A, Engler JA, Xu H, Cherry AM, Kay MA. Molecular analysis of chromosomal rearrangements in mammalian cells after  $\phi$ C31-mediated integration. *Hum. Gene Ther*. 2006; 17:1077–1094. [PubMed: 17069535]
37. Liu J, Jeppesen I, Nielsen K, Jensen TG. PhiC31 integrase induces chromosomal aberrations in primary human fibroblasts. *Gene Ther*. 2006; 13:1188–1190. [PubMed: 16672982]
38. Liu J, Skjorringe T, Gjetting T, Jensen TG. PhiC31 integrase induces a DNA damage response and chromosomal rearrangements in human adult fibroblasts. *BMC. Biotechnol*. 2009; 9:31. [PubMed: 19341467]

39. Iwai Y, et al. Axon patterning requires DN-cadherin, a novel neuronal adhesion receptor, in the *Drosophila* embryonic CNS. *Neuron*. 1997; 19:77–89. [PubMed: 9247265]
40. Vandaele C, Coulon-Bublex M, Couble P, Durand B. *Drosophila* regulatory factor X is an embryonic type I sensory neuron marker also expressed in spermatids and in the brain of *Drosophila*. *Mech. Dev.* 2001; 103:159–162. [PubMed: 11335126]
41. Bodily KD, Morrison CM, Renden RB, Broadie K. A novel member of the Ig superfamily, turtle, is a CNS-specific protein required for coordinated motor control. *J. Neurosci.* 2001; 21:3113–3125. [PubMed: 11312296]
42. Brown NH, et al. Talin is essential for integrin function in *Drosophila*. *Dev. Cell.* 2002; 3:569–579. [PubMed: 12408808]
43. Yao CK, et al. A synaptic vesicle-associated Ca<sup>2+</sup> channel promotes endocytosis and couples exocytosis to endocytosis. *Cell.* 2009; 138:947–960. [PubMed: 19737521]
44. Negre N, et al. A cis-regulatory map of the *Drosophila* genome. *Nature.* 2011; 471:527–531. [PubMed: 21430782]
45. Gohl DM, et al. A versatile in vivo system for directed dissection of gene expression patterns. *Nat. Methods.* 2011; 8:231–237. [PubMed: 21473015]
46. Wesolowska N, Rong YS. The past, present and future of gene targeting in *Drosophila*. *Fly. (Austin.)* 2010; 4:53–59. [PubMed: 20139712]
47. Venken KJ, He Y, Hoskins RA, Bellen HJ. P[acman]: a BAC transgenic platform for targeted insertion of large DNA fragments in *D. melanogaster*. *Science.* 2006; 314:1747–1751. [PubMed: 17138868]
48. Venken KJ, et al. Versatile P[acman] BAC libraries for transgenesis studies in *Drosophila melanogaster*. *Nat. Methods.* 2009; 6:431–434. [PubMed: 19465919]
49. Klinakis AG, Loukeris TG, Pavlopoulos A, Savakis C. Mobility assays confirm the broad host-range activity of the Minos transposable element and validate new transformation tools. *Insect Mol. Biol.* 2000; 9:269–275. [PubMed: 10886410]
50. Groth AC, Olivares EC, Thyagarajan B, Calos MP. A phage integrase directs efficient site-specific integration in human cells. *Proc. Natl. Acad. Sci. U. S. A.* 2000; 97:5995–6000. [PubMed: 10801973]
51. Hodges D, Bernstein SI. Suboptimal 5' and 3' splice sites regulate alternative splicing of *Drosophila melanogaster* myosin heavy chain transcripts in vitro. *Mech. Dev.* 1992; 37:127–140. [PubMed: 1498040]
52. Okada A, Lansford R, Weimann JM, Fraser SE, McConnell SK. Imaging cells in the developing nervous system with retrovirus expressing modified green fluorescent protein. *Exp. Neurol.* 1999; 156:394–406. [PubMed: 10328944]
53. Horton RM, Hunt HD, Ho SN, Pullen JK, Pease LR. Engineering hybrid genes without the use of restriction enzymes: gene splicing by overlap extension. *Gene.* 1989; 77:61–68. [PubMed: 2744488]
54. Pavlopoulos A, Berghammer AJ, Averof M, Klingler M. Efficient transformation of the beetle *Tribolium castaneum* using the Minos transposable element: quantitative and qualitative analysis of genomic integration events. *Genetics.* 2004; 167:737–746. [PubMed: 15238525]
55. Apitz H, et al. Identification of regulatory modules mediating specific expression of the roughest gene in *Drosophila melanogaster*. *Dev. Genes Evol.* 2004; 214:453–459. [PubMed: 15278452]
56. Raymond CS, Soriano P. High-Efficiency FLP and  $\phi$ C31 Site-Specific Recombination in Mammalian Cells. *PLoS. ONE.* 2007; 2:e162. [PubMed: 17225864]
57. Shaner NC, et al. Improved monomeric red, orange and yellow fluorescent proteins derived from *Discosoma* sp. red fluorescent protein. *Nat. Biotechnol.* 2004; 22:1567–1572. [PubMed: 15558047]
58. Pedelacq JD, Cabantous S, Tran T, Terwilliger TC, Waldo GS. Engineering and characterization of a superfolder green fluorescent protein. *Nat. Biotechnol.* 2006; 24:79–88. [PubMed: 16369541]
59. Ai HW, Shaner NC, Cheng Z, Tsien RY, Campbell RE. Exploration of new chromophore structures leads to the identification of improved blue fluorescent proteins. *Biochemistry.* 2007; 46:5904–5910. [PubMed: 17444659]

60. Shaner NC, et al. Improving the photostability of bright monomeric orange and red fluorescent proteins. *Nat. Methods*. 2008; 5:545–551. [PubMed: 18454154]
61. Smith AT, et al. Expression of a synthetic gene for horseradish peroxidase C in *Escherichia coli* and folding and activation of the recombinant enzyme with Ca<sup>2+</sup> and heme. *J. Biol. Chem.* 1990; 265:13335–13343. [PubMed: 2198290]
62. Gurskaya NG, et al. Engineering of a monomeric green-to-red photoactivatable fluorescent protein induced by blue light. *Nat. Biotechnol.* 2006; 24:461–465. [PubMed: 16550175]
63. Chudakov DM, Lukyanov S, Lukyanov KA. Using photoactivatable fluorescent protein Dendra2 to track protein movement. *Biotechniques*. 2007; 42:553, 555, 557. [PubMed: 17515192]
64. Bulina ME, et al. A genetically encoded photosensitizer. *Nat. Biotechnol.* 2006; 24:95–99. [PubMed: 16369538]
65. Martin BR, Giepmans BN, Adams SR, Tsien RY. Mammalian cell-based optimization of the biarsenical-binding tetracysteine motif for improved fluorescence and affinity. *Nat. Biotechnol.* 2005; 23:1308–1314. [PubMed: 16155565]
66. Schmidt TG, Koepke J, Frank R, Skerra A. Molecular interaction between the Strep-tag affinity peptide and its cognate target, streptavidin. *J. Mol. Biol.* 1996; 255:753–766. [PubMed: 8636976]
67. Terpe K. Overview of tag protein fusions: from molecular and biochemical fundamentals to commercial systems. *Appl. Microbiol. Biotechnol.* 2003; 60:523–533. [PubMed: 12536251]
68. Evan GI, Lewis GK, Ramsay G, Bishop JM. Isolation of monoclonal antibodies specific for human c-myc proto-oncogene product. *Mol. Cell Biol.* 1985; 5:3610–3616. [PubMed: 3915782]
69. Wilson IA, et al. The structure of an antigenic determinant in a protein. *Cell*. 1984; 37:767–778. [PubMed: 6204768]
70. Dougherty WG, Cary SM, Parks TD. Molecular genetic analysis of a plant virus polyprotein cleavage site: a model. *Virology*. 1989; 171:356–364. [PubMed: 2669323]
71. Hackbarth JS, et al. S-peptide epitope tagging for protein purification, expression monitoring, and localization in mammalian cells. *Biotechniques*. 2004; 37:835–839. [PubMed: 15560139]
72. Southern JA, Young DF, Heaney F, Baumgartner WK, Randall RE. Identification of an epitope on the P and V proteins of simian virus 5 that distinguishes between two isolates with different biological characteristics. *J. Gen. Virol.* 1991; 72:1551–1557. [PubMed: 1713260]
73. Parks AL, et al. Systematic generation of high-resolution deletion coverage of the *Drosophila melanogaster* genome. *Nat. Genet.* 2004; 36:288–292. [PubMed: 14981519]
74. Ferguson K, Long H, Cameron S, Chang WT, Rao Y. The conserved Ig superfamily member Turtle mediates axonal tiling in *Drosophila*. *J. Neurosci.* 2009; 29:14151–14159. [PubMed: 19906964]
75. Al-Anzi B, Wyman RJ. The *Drosophila* immunoglobulin gene turtle encodes guidance molecules involved in axon pathfinding. *Neural Dev.* 2009; 4:31. [PubMed: 19686588]
76. Tear G, et al. commissureless controls growth cone guidance across the CNS midline in *Drosophila* and encodes a novel membrane protein. *Neuron*. 1996; 16:501–514. [PubMed: 8785048]
77. Nern A, et al. An isoform-specific allele of *Drosophila* N-cadherin disrupts a late step of R7 targeting. *Proc. Natl. Acad. Sci. U. S. A.* 2005; 102:12944–12949. [PubMed: 16123134]
78. Stapleton M, et al. A *Drosophila* full-length cDNA resource. *Genome Biol.* 2002; 3 RESEARCH0080.
79. Lecuyer E, Parthasarathy N, Krause HM. Fluorescent in situ hybridization protocols in *Drosophila* embryos and tissues. *Methods Mol. Biol.* 2008; 420:289–302. [PubMed: 18641955]
80. Lehmann R, Tautz D. In situ hybridization to RNA. *Methods Cell Biol.* 1994; 44:575–598. [PubMed: 7535885]

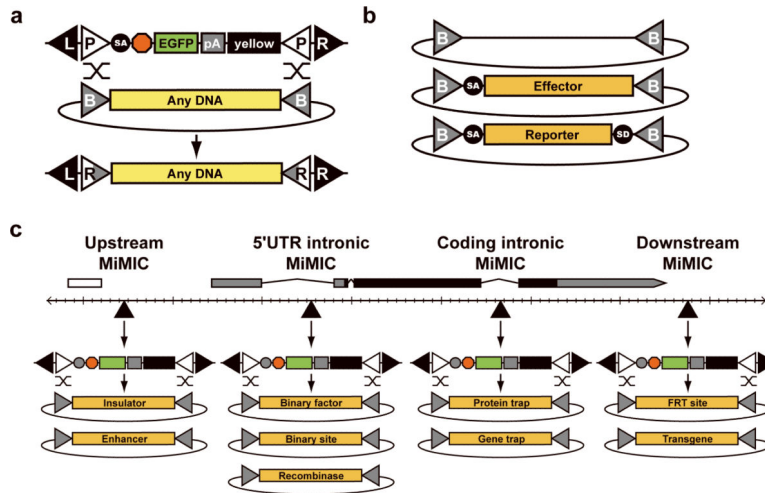


**Figure 1. The MiMIC transposon system**

(a) MiMIC consists of two *Minos* inverted repeats (L and R), two inverted  $\Phi$ C31 *attP* sites (P), a gene trap cassette consisting of a splice acceptor site (SA) followed by stop codons in all three reading frames, and the EGFP coding sequence with a polyadenylation signal (pA), and the *yellow*<sup>+</sup> marker. The sequence between the *attP* sites can be replaced via RMCE, resulting in two *attR* sites (R). (b) Three *attB* plasmids for RMCE: a correction plasmid consisting of a multiple cloning site, a gene-trap plasmid consisting of a SA fused to a downstream effector, and a protein-trap plasmid consisting of a reporter flanked by SA and SD sites. (c) Various MiMIC insertions in a hypothetical gene with regulatory element (white), 5' and 3' untranslated regions (grey), and coding regions (black), that can be used for several applications as indicated.

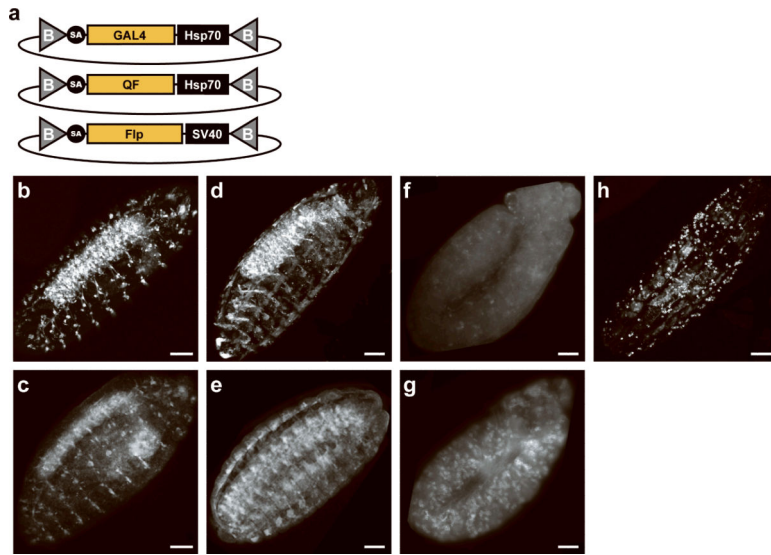


**Figure 2. Binary expression and lineage analysis with MiMIC insertions**

(a) Gene-trap cassettes that incorporate the GAL4 or QF transactivators for binary activation, and the Flp recombinase for fate mapping. Live imaging (b, d) and confocal microscopy analysis using an anti-Cherry antibody (c, e) of the expression domain revealed by GAL 4 inserted in *gogo* (b,c ) or the *caps* locus (d,e). The expression domain of *MYPT-75D* revealed by GAL4 (f) or QF (g) integrated in *MYPT-75D*. Live imaging of the GAL4 expression pattern revealed by GAL4 inserted in *BM-40-SPARC* (h). Scale bars are 50 μm.



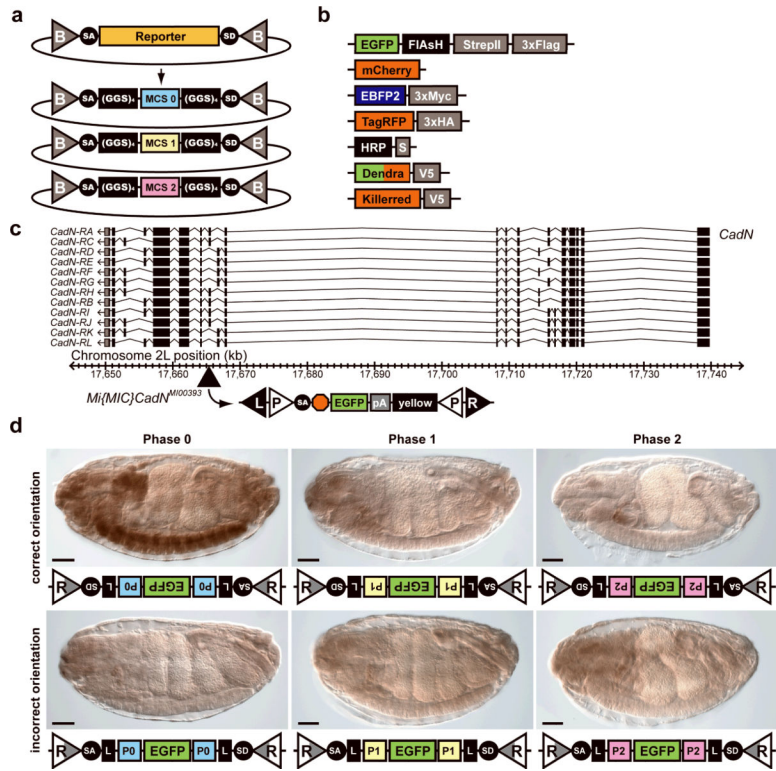


**Figure 3. Protein trapping with MiMIC insertions**  
**(a)** For each protein-trap cassette, three versions were constructed corresponding to the three intron phases (0, 1 and 2). (GGS)<sub>4</sub>, flexible peptide linker sequence encoding a GlyGlySer quadruplet tandem repeat. **(b)** Tag and multi-tag cassettes expressing the indicated reporters are shown. **(c)** A 100 kb genomic region containing *CadN* is shown. The location of the *Mi(MIC)CadN<sup>M100393</sup>* insertion in a phase 0 coding intron is indicated. **(d)** Integration of a phase 0 EGFP-FIAsh-StrepII-3×Flag cassette (EGFP) in the indicated orientation and intron phase. L, (GGS)<sub>4</sub> linker; R, (*attR*); P0, splice phase 0; P1, splice phase 1; P2, splice phase 2. Scale bars are 50 μm.

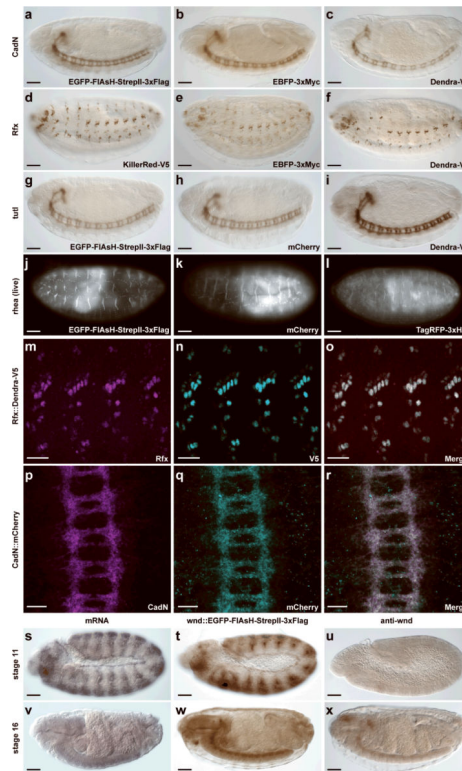


#### Figure 4. Expression analyses of tagged proteins

(a–i) Detection of different protein-trap alleles of three genes using antibodies against several epitopes and diaminobenzidine/peroxidase (DAB) staining. In each panel, the tag or multi-tag is indicated in the lower right; the portion of the tag that was used as the antigen is italicized. (a–c) Expression of tagged CadN during embryonic stage 15: staining with (a) anti-EGFP, (b) anti-EBFP (c) anti-Dendra. (d–f) Expression of tagged Rfx in stage 15 embryos: staining with (d) anti-V5, (e) anti-EBFP (f) anti-Dendra. (g–i) Expression of tagged Tutl in the ventral nerve cord of stage 15 embryos: staining with (g) anti-EGFP, (h) anti-mCherry, (i) anti-Dendra. (j–l) Fluorescent detection of different protein-trap alleles in live stage 17 embryos expressing tagged Rhea: (j) EGFP (k) mCherry (l) TagRFP. (m–r) Co-localization of protein traps and endogenous proteins in stage 15 embryos for Rfx (m–o) and CadN (p–r). Anti-Rfx staining (m), anti-V5 staining (n), and co-staining (o) in an Rfx: :Dendra-V5 trap. Anti-CadN staining (p), anti-mCherry staining (q), and co-staining (r) in a CadN: :mCherry trap. (s–x) Novel expression detected using protein traps. (s,v) Expression of *wnd* detected using mRNA *in situ* hybridization. (t,w) Expression of Wnd detected by anti-EGFP staining of an EGFP-FIAsH-StrepII-3×Flag trap and (u,x) anti-Wnd staining during embryonic stages 11 (s–u) and 16 (v–x). Scale bars are 50  $\mu$ m (a–l, s–x) and 20  $\mu$ m (m–r).

**Table 1**

**Protein-trapping experiments**

MiMIC insertions in six genes were tagged with different protein-trap cassettes using RMCE. For each insertion, gene, MiMIC line, gene-trap status, associated lethality and intron phase are indicated. For each RMCE experiment, tag component, total lines, number of expressing lines, percentage of expressing lines, and lethality (viable (V), >5% viable homozygotes), lethal (L), not applicable (NA)) are indicated.

		Insertion						RMCE					
Gene	MiMIC	Gene trap	Lethality	Phase	Tag <sup>d</sup>	Total	Expression	%	Lethality				
<i>Rfx</i>	MI00053	YES	Lethal	1	EGFP	1	0	0%	NA				
					mCherry	2	1	50%	L				
					EBFP	2	1	50%	V				
					3xHA	2	1	50%	V				
					S peptide	5	2	40%	2L				
					Dendra	6	5	83%	5V				
					V5	3	3	100%	2V/L				
<i>tut</i>	MI00290	YES	Lethal	1	EGFP	4	3	75%	3V				
					mCherry	6	2	33%	2V				
					EBFP	3	2	67%	2V				
					3xHA	1	0	0%	NA				
					S peptide	5	3	60%	3V				
					Dendra	5	2	40%	2V				
					V5	5	2	40%	2L				
<i>rhea</i>	MI00296	NO	Viable	0	EGFP	5	3	60%	V/2L				
					mCherry	4	2	50%	V/L				
					EBFP	6	3	50%	2V/L				
					3xHA	5	2	40%	2V				
					S peptide	5	0	0%	NA				
					Dendra	6	4	67%	3V/L				
					V5	6	4	67%	4V				
<i>comm</i>	MI00380	YES	Lethal	1	EGFP	7	2	29%	V/L				

Insertion							RMCE			
Gene	MiMIC	Gene trap	Lethality	Phase	Tag <sup>a</sup>	Total	Expression	%	Lethality	
					mCherry	3	2	67%	V/L	
					EBFP	5	2	40%	2L	
					3×HA	2	1	50%	L	
					S peptide	5	1	20%	L	
					Dendra	5	1	20%	L	
					V5	5	4	80%	4L	
<i>CadN</i>	MI00393	NO	Viable	0	EGFP	5	3	60%	3V	
					mCherry	2	1	50%	V	
					EBFP	4	2	50%	V/L	
					3×HA	4	1	25%	V	
					S peptide	3	1	33%	V	
					Dendra	4	2	50%	2V	
					V5	3	1	33%	V	
<i>wnd</i>	MI00494	YES	Lethal	2	EGFP	5	5	100%	5L	
					mCherry	3	1	33%	L	
					EBFP	3	1	33%	L	
					3×HA	3	0	0%	NA	
					S peptide	4	3	75%	3L	
					Dendra	3	1	33%	V	
					V5	1	0	0%	NA	
Total						166	80	48%		

<sup>a</sup>Tag components of multi-tags used for expression analysis: EGFP (eGFP-FlAsH-StrepII-3×Flag), mCherry (mCherry), EBFP (eBFP-3×Myo), 3×HA (TagRFP-3×HA), S peptide (HRP-S peptide), Dendra (Dendra-V5), V5 (Killerred-V5).